J Solid State Electrochem (2012) 16:3635–3641
DOI 10.1007/s10008-012-1796-2

ORIGINAL PAPER

KCl-assisted, chemically reduced graphene oxide for high-performance supercapacitor electrodes

Rixiong Chen · Shuhui Yu · Rong Sun · Wenhu Yang · Yubao Zhao

Received: 6 February 2012 / Revised: 11 June 2012 / Accepted: 12 June 2012 / Published online: 27 June 2012

Abstract Graphene with highly flaky state has been successfully prepared through chemical reduction process with the assistance of potassium chloride (KCl) to enhance the ionic strength in the aqueous solution. The microstructure of graphene sheets (GS) prepared in different solutions was compared and the effect of the KCl on the dispersion of GS was investigated. The buoyancy and repulsive force from the ions in the solution were effective to prevent the graphene sheets from agglomerating with each other. SEM and TEM images showed that the graphene reduced in KCl solution has kept the highly flaky state whereas the graphene reduced in pure water has curled and re-stacked together. As for supercapacitor electrode application, the highly flaky graphene showed much higher specific capacitance than the agglomerated one in 1 M Li_2SO_4 electrolyte. The more accessible surface of the graphene reduced with KCl assistance effectively enhanced the electric double layer capacitance.

Keywords Graphene · KCl · Ionic strength · Agglomeration · Supercapacitor

Introduction

Graphene, a new class of carbon material consisting of a sp^2 atom network, has attracted extensive research interests due to its extraordinary mechanical, electrical and thermal properties [1–4]. It has been expected to be applied in nanoelectronics [5, 6], sensors [7, 8], supercapacitors [9–11], transparent electrodes [12–14], and transistors [15]. In light of the fact that the graphene has many superior features and functions, a large amount of this two-dimensional nanomaterial is desired in industrialized manufacture. However, high quality and large-scale preparation of the graphene with uniform thickness still faces many challenges [16, 17].

Graphene has been prepared in several methods. In the year 2004, mechanical exfoliation of graphene was reported [18] and then appeared chemical vapor deposition [19] and chemical reduction of graphene oxide. The chemical reduction of graphene oxide generally employed hydrazine [20], dimethylhydrazine [21], hydrobromic acid [22] (or hydroiodic acid [23]) or $NaBH_4$ [24] as the reducing agent. However, when these reducing agents were used in liquid state, the reduced graphene generally tended to agglomerate into big lumps. To solve this problem, surfactants were used to stabilize the graphene dispersion during the reducing process [25–27]. But it was still hard to acquire graphene with flaky state in mass weight and the excess use of surfactants would bear on the environment.

As a prospect of the supercapacitor electrode material, graphene has shown a specific capacitance as high as 348 F g^{-1} in 1 M H_2SO_4 [22]. Although the specific capacitance of the graphene in acid or alkaline electrolyte has shown much higher values than that in neutral electrolyte which is normally lower than 100 F g^{-1} [28], it should be noted that the latter is preferred in view of the safety and environment protection.

In this paper, we report an effective way to produce graphene with highly flaky state by adding KCl to assist enhancing ionic strength of the aqueous solution and using hydrazine as reducing agent. The effect of KCl on the dispersion of the graphene sheets obtained through the

R. Chen · S. Yu (✉) · R. Sun (✉) · W. Yang
Shenzhen Institutes of Advanced Technology, Chinese Academy of Sciences and the Chinese University of Hong Kong, Shenzhen 518055, China
e-mail: yuushu@gmail.com
e-mail: rong.sun@siat.ac.cn

R. Chen · Y. Zhao
School of Chemistry and Chemical Engineering, University of South China, Hengyang 421001, China

chemical reduction of graphene oxide was investigated. The electrochemical properties of the derived graphene have been characterized for supercapacitor application in neutral Li_2SO_4 electrolyte.

Experimental

Synthesis of graphene sheets

Graphite oxide (GO) was prepared from graphite powder (GP; ≤30 μm, Sinopharm Chemical Reagent Co., Ltd) by a modified Hummers method [29]. In a typical process, 5 g of GP was first pre-oxidized in a three-neck flask at 80 °C for 4 h with 30 ml concentrated H_2SO_4 (98 %). After cooling down to room temperature, the three-neck flask was transferred to an ultrasonic cleaner and sonicated for 2 h (400 W, 40 MHz). The mixture was diluted and washed with deionized (DI) water. After vacuum drying at 70 °C for 24 h, the pre-oxidized GP was attained which was then further oxidized with Hummers method. In a typical process, the pre-oxidized GP was added to the three-neck flask again at a low temperature (<10 °C); 100 ml concentrated sulfuric acid (98 %) and 2.5 g sodium nitrate were used to oxidize the pre-oxidized GP for 30 min. After adding 20 g potassium permanganate, the temperature was increased to 35 °C for another 30 min. The slurry was slowly diluted by about 200 ml DI water to get brown dispersion. Then the temperature was increased to 98 °C and kept at this temperature for about 10 min. The color of the dispersion was changed to brown-yellow. Then 75 ml water was added to the solution to dilute the dispersion again. After reducing the by-producing manganese dioxide with 30 ml of H_2O_2 (30 %), the dispersion was centrifuged at a speed of 7,200 rpm. Diluted HCl (37.5 % concentrated hydrochloric acid 1:10 diluted with water in volume) and DI water were further used to wash the slurry.

The GO was reduced with hydrazine hydrate in an oil bath reflux apparatus with a water-cooled condenser at 100 °C for 4 h. In a typical procedure, 0.5 g GO was ultrasonically exfoliated in 500 ml DI water for 2 h. Then 37.28 g (0.50 mol) KCl solid powder was added to the solution and stirred to get floccose exfoliated GO dispersion; 5.5 ml 80 % hydrazine hydrate was added to the solution as reducing agent. The as-prepared graphene sheet (GS) was filtered and washed with water. Finally, the GS was freezing-dried for 24 h and the graphene sheet in KCl (aq) (GSK) sample was then obtained. For a comparative experiment, the GO was reduced in pure water to attain the graphene sheet in water (GSW) with the same procedure.

Characterization of the GS samples

Morphological features of the GS were studied using a scanning electron microscopy (SEM, Hitachi S-4800 equipped with an energy dispersive X-ray (EDX) spectroscope) and a transmission electron microscopy (TEM, JEOL -2100 F, 200 keV). The thermogravimetric analysis (TGA) weight loss was tested on a Q600 under N_2 flow with a temperature increasing scan rate of 10 °C/min. The XRD results were attained from a Rigaku SmartLab (Cu Kα, λ= 0.15406 nm) and Raman data were measured on a Renishaw InVia Raman microscope equipped with an excitation laser at 785 nm, respectively. Brunauer–Emmett–Teller (BET) surface areas were measured on a micromeritics ASAP 2020 system using nitrogen adsorption at 77 K.

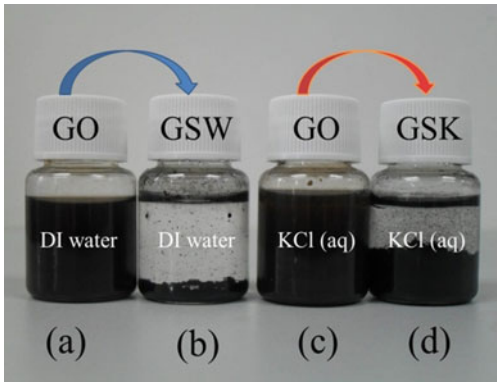

Fig. 1 Photograph of exfoliated GO and GS in different solutions. The *arrows* show shat the exfoliated GO is reduced to GS in DI water and KCl (aq), respectively

Preparation of supercapacitor electrodes and electrochemical measurements

The as-prepared GS sample was mixed with poly(tetrafluoroethylene) (PTFE, 60 % in water) by a mass ratio of 9:1 using ethanol as solvent. After ultrasonic mixing up for 20 min, the slurry was coated onto 1.5 cm diameter nickel foam wafers and dried at 70 °C for 5 h. After the electrodes were pressed with 20 MPa, one of the Ni foam electrodes was used as the working electrode where a platinum foil and

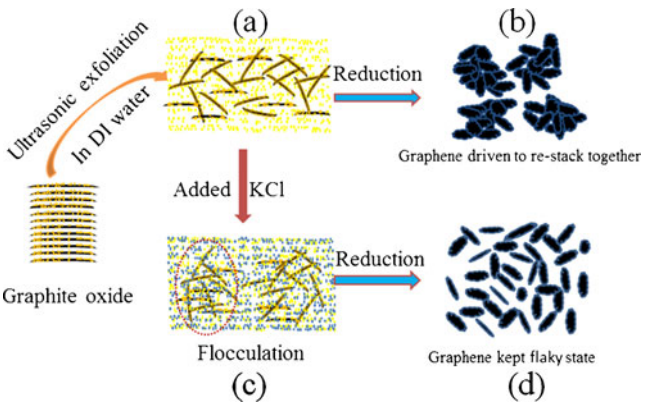

Fig. 2 Schematic illustration of the GO exfoliated and reduced to GS

Table 1 Elements' percent of the GO, GOK, GSW, GSK (note: GOK means exfoliated GO in KCl solution)

Element	GO		GOK		GSW		GSK	
	Weight%	Atomic%	Weight%	Atomic%	Weight%	Atomic%	Weight%	Atomic%
C K	64.32	70.60	53.52	65.82	78.96	83.33	82.89	87.12
O K	35.68	29.40	29.76	27.47	21.04	16.67	15.76	12.44
K K	–	–	6.80	2.57	–	–	1.23	0.40
Cl K	–	–	9.92	4.14	–	–	0.12	0.04
Totals	100.00							

Ag/AgCl electrode as the counter and reference electrodes for cyclic voltammograms (CV) measurements on a Zennium electrochemical workstation. Two electrodes were packaged in a 2032 test cell mold (Tianjin Liangnuo scientific Co. Ltd.) and a porous nonwoven cloth was used as separator for the galvanostatic charge/discharge testing on a LAND cell tester.

Results and discussion

Effect of KCl on the GS preparation process

Figure 1 presents the photograph of exfoliated GO reduced to GS in DI water and KCl (aq), respectively. The GS in bottle (b) has deposited to the bottom. In contrast, when GO was reduced in KCl solution, most of the derived GS was floating in the solution (bottle (d)). The prominent difference indicates that KCl substantially improves the dispersion of GS through the reduction process.

In order to illustrate the effect of KCl on the formation of the highly dispersed GS, a schematic process is proposed, as shown in Fig. 2, in which (a)–(b) indicates the formation process of GS in DI water and (a)–(b)–(c) in KCl solution. When GO is exfoliated in DI water, a homogeneous yellow-brown solution is attained as shown in Fig. 2a and b shows the universal phenomenon that after the exfoliated GO is chemically reduced, the obtained GS agglomerates severely. In contrast, as KCl is introduced to the process, the salt solution with high ionic strength is obtained. As a result, the exfoliated GO could stably flocculate and float in the solution, as shown in Fig. 2c. Owing to the high ionic strength in the KCl solution, the K^+ ion could intercalate easily into the layer interspace of the GO and form new bonds with the oxygen groups. This speculation could be perceived by the EDX results of the GSK sample that the atomic amount of potassium is almost ten times of the chlorine as shown in Table 1. Results also show that the C/O ratios in the GSK and GSW are 7:1 and 5:1, respectively, indicating that less oxygens are left in GSK than in GSW. For GSK, the left amount of K is much higher than that of Cl (0.40 % vs. 0.04 %), indicating that K^+ is more possible to interact with the oxygen groups in GO. As shown in Fig. 2d, after it was reduced to GSK which has less oxygenic groups than the GO, the as-prepared graphene sample could float in the KCl solution. The repulsive force arising from the K^+ ions on the plane surfaces of GO causes the flaky GO to detach away from each other. Due to the high ionic strength and buoyancy of the solution, the graphene sheets could float independently. As a result, the GSK could keep a stretched surface in the salt solution and less agglomeratation could occur than the GSW. The BET surface area of the GSK is 676.5 m^2/g while the GSW is only 372.7 m^2/g.

Figure 3 shows the TGA curves of the GO, GSW and GSK. The weight of GO has decreased by about 43.8 % before 300 °C and both of the GSW and GSK have decreased less than 1 % at this temperature. The weight loss of the GSK or GSW is much smaller than that of GO. It suggests that the GO has been reduced to GS in KCl (aq) or water. The slight deviation of the weight loss at high temperature can be attributed to the oxygen level of the reduced GS that is gasifiable.

Microstructure characterization

Figure 4 shows the typical SEM images of GSK: (a) and (b), and GSW: (c) and (d). Figure 4a shows the typical plane GS at low amplified magnification after freezing dry. As shown in Fig. 4b at high magnification, most of the GSK presents

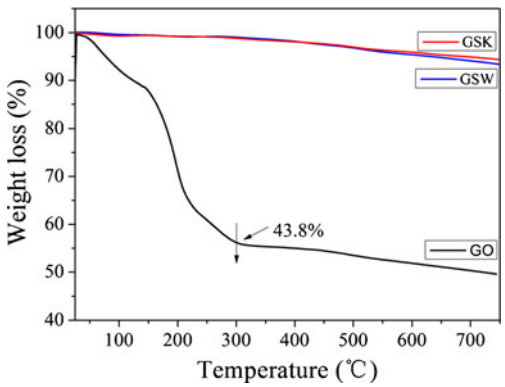

Fig. 3 The TGA curves of the GO, GSK, and GSW

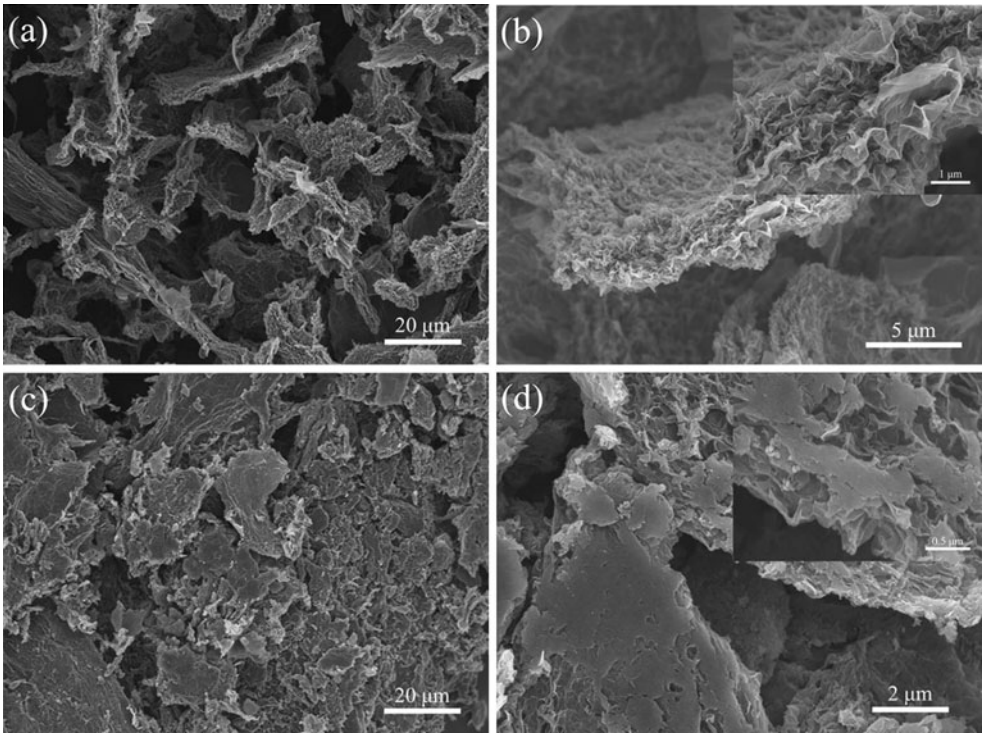

Fig. 4 SEM images of the GSK: **a** and **b**, and GSW: **c** and **d** at different magnifications (the inserted ones in **b** and **d** show clearer difference between the two types of GS at higher magnification)

flaky state and stretches like flowers which are not agglomerating. While the GSW shown in Fig. 4c and d as well as in the inserted image, is re-stacking and looks like bricks at high magnification.

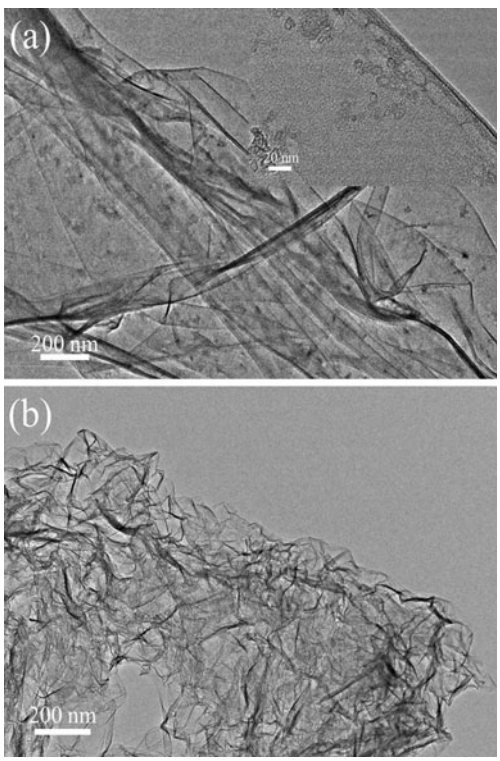

Fig. 5 The TEM images of the GSK (**a**) (the *inserted HRTEM image* shows the edge of one flaky GSK) and GSW (**b**)

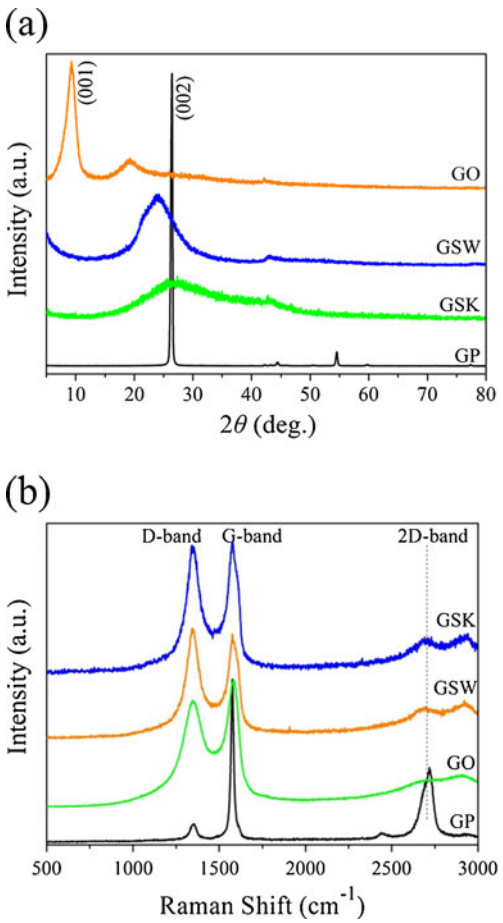

Fig. 6 X-ray diffraction patterns (**a**) and Raman spectrums (**b**) of GP, GO, GSW, and GSK

TEM images in Fig. 5 show clearer difference between the typical GS reduced in KCl (aq) (a) and water (b). In Fig. 5a and the inserted image (up-right corner), the GSK shows superior flaky state and the film is transparent and stretching. Although the films are slightly winded, it is easy to identify the edge and contour. In contrast, the GSW in Fig. 5b is severely wrapped to each other and shows no obvious edge and contour. The results indicate that in the salt solution with high ionic strength, the reduced GS can hold its flaky state and prevent caking.

Figure 6a shows the XRD patterns of GP, GO, GSW and GSK. The GP shows a strong (002) peak at 26.4° while a (001) peak at 9.3° with strong intensity appears for GO. For GSW, a high-intensity and triangle peak appears around 23.8°. It is worth noting that the (002) peak of GSK is located at 26.5° which is close to the peak of the graphite [30]. The low intensity of the peak indicates that when it was reduced in KCl aqueous, the GS could keep its flaky state with fewer stacking structure than that reduced in water. Furthermore, because of the curly state for the GSW, the inner oxygenic groups are not sufficiently reduced resulting in the shift of the (002) peak to a smaller 2θ angle,

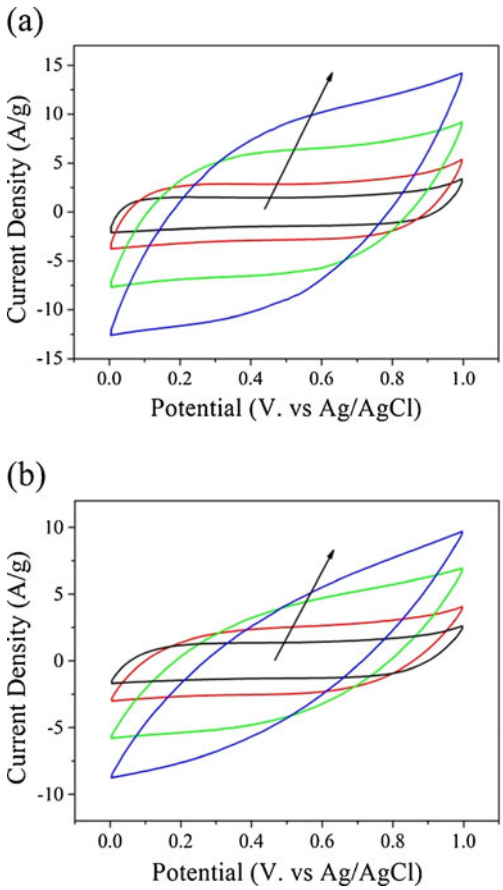

Fig. 7 CV curves of the GSK (**a**) and GSW (**b**) at different scan rates of 10, 20, 50, and 100 mV s^{-1} (increased directly as the *arrows*)

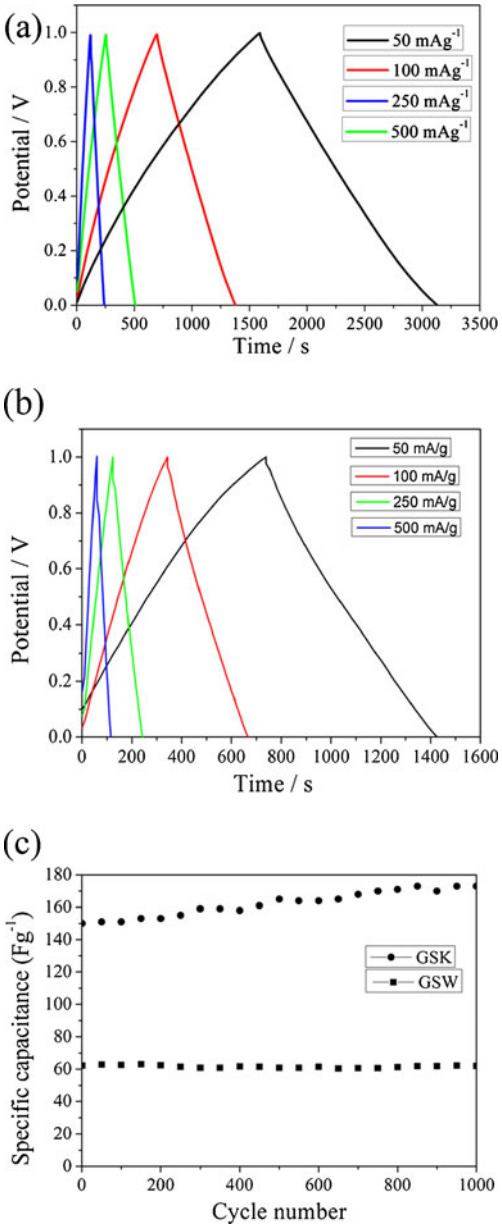

Fig. 8 Galvanostatic charge and discharge curves of the GSK (**a**) and GSW (**b**) supercapacitor at current densities of 50, 100, 250, and 500 mA/g, and the specific capacitance of 1,000 cycles (**c**), the inserted ones are five galvanostatic charge/discharge curves of GSK and GSW at the highest specific capacitance

as supported by the EDX analysis. Figure 6b shows the typical Raman spectrums of the GP, GO, GSW and GSK. The two dominant peaks are assigned to D-band at 1,350 cm^{-1} and G-band at about 1,575 cm^{-1}. And the weak peak at 2,709 cm^{-1} is ascribed to 2D-band. The G-band of GP is sharper and the intensity is higher than D-band whereas the intensity of 2D-band is also strong. After the GP is oxidized to GO, the D-band is still lower than the G-band. However, for both GSK and GSW, the intensity of D-bands is strengthened and close to the G-bands. Because the D-

band and G-band corresponds respectively to the occurrence of the sp^2 C with defects and the zone center E2g mode relates to phonon vibration in sp^2 carbon atoms [31], this change well demonstrates that the GP has been exfoliated to GS flakes. Amazing for 2D-band, it has been weakened after going through the experimental process.

Electrochemical properties

The CV and galvanostatic charge/discharge curves are usually used to characterize the performance of the supercapacitor. Figure 7 shows the CV curves of the GSK (a) and GSW (b) as supercapacitor electrodes measured at different scan rates of 10, 20, 50, and 100 mV s^{-1} increased directly as indicated by the arrows in 1 M Li_2SO_4 electrolyte. The CV curves do not show any obvious faradaic properties in this electrolyte. The measurement for the highly flaky GSK at 50 mV s^{-1} is much closer to a quasi-rectangular shape with small distortion, indicating that it has a more ideal capacitive property than the GSW [22]. Correspondingly, the CV curves of the highly flaky GSK show a much larger area which means that it can provide better electric double layer capacitance than the agglomerated GSW.

The galvanostatic charge/discharge performance and specific capacitance of the two GS samples are shown in Fig. 8. All the curves are linear and nearly symmetrical at various current densities from 50 to 500 mA g^{-1}. For practical application, we measured the specific capacitance of the GS with two-electrode supercapacitor. The specific capacitance was calculated using the following equation:

$$C_{\mathrm{m}} = \frac{2I\Delta t}{m\Delta V}$$

where I is the discharge current density, Δt is the time elapsed for the discharge, m is the mass of the GS in one electrode and ΔV is the voltage interval of the discharge (excluding the iR drop). As shown in Fig. 8a and b, the GSK has shown much longer charge/discharge time for one cycle than the GSW at the same discharge current density, which means that it could have much higher specific capacitance. The cycle characterization and the specific capacitance of the two samples are shown in Fig. 8c. As shown in the figure, the capacitance of GSW is only about 64 F g^{-1} which keeps up to 97 % after 1,000 cycles. But the cyclic performance of GSK shows about 150 F g^{-1} at the first galvanostatic charge/discharge cycle and then increases to 173 F g^{-1} at the 1,000th cycle. Since the contactable area of the GS for the electrolyte ions is one of the most important factors to affect the electric double layer capacitance, the high flaky state GS which is stretching like flowers demonstrates much more passages and then higher specific capacitance than the curled and re-stacked one like sticks.

Conclusions

In this study, high ionic strength KCl solution has been introduced to the chemical reduction of graphene oxide. We found that the derived GS could keep its flaky state and stretch like flowers after the reduction and drying process. In contrast to that obtained in the KCl solution, the GS reduced in pure water has re-stacked and agglomerated together. Because of the high concentration of the ions in the solution, the buoyancy and repulsive force has prevented the GS from re-stacking to each other when and after it was reduced. The highly flaky GS has shown much larger specific capacitance than the agglomerated GS in 1 M Li_2SO_4 electrolyte. This study provides a guidance in obtaining stretched graphene sheets with large surface area, which demonstrates high electric double layer capacitance when being used as supercapacitor electrodes.

Acknowledgments This work was financially supported by National Natural Science Foundation of China (No. 50807038 and 20971089), and the program for "Shenzhen Outstanding Young Talent" (Contract No. JC201005270367A).

References

1. Lee C, Wei X, Kysar JW, Hone J (2008) Science 321:385–388
2. Yoo E, Kim J, Hosono E, Zhou H, Kudo T, Honma I (2008) Nano Lett 8:2277–2282
3. Balandin AA, Ghosh S, Bao W, Calizo I, Teweldebrhan D, Miao F, Lau CN (2008) Nano Lett 8:902–907
4. Compton OC, Dikin DA, Putz KW, Brinson LC, Nguyen ST (2010) Adv Mater 22:892–896
5. Westervelt RM (2008) Science 320:324–325
6. Xuan Y, Wu YQ, Shen T, Qi M, Capano MA, Cooper JA, Ye PD (2008) Appl Phys Lett 92:13101–13103
7. Dan Y, Lu Y, Kybert NJ, Luo Z, Johnson ATC (2009) Nano Lett 9:1472–1475
8. Fowler JD, Allen MJ, Tung VC, Yang Y, Kaner RB, Weiller BH (2009) ACS Nano 3:301–306
9. Stoller MD, Park S, Zhu Y, An J, Ruoff RS (2008) Nano Lett 8:3498–3502
10. Fu C, Kuang Y, Huang Z, Wang X, Yin Y, Chen J, Zhou H (2011) J Solid State Electr 15:2581–2585
11. Wang Y, Shi Z, Huang Y, Ma Y, Wang C, Chen M, Chen Y (2009) J Phys Chem C 113:13103–13107
12. Kim KS, Zhao Y, Jang H, Lee SY, Kim JM, Kim KS, Ahn J, Kim P, Choi J, Hong BH (2009) Nature 457:706–710
13. Wu J, Agrawal M, Becerril HA, Bao Z, Liu Z, Chen Y, Peumans P (2010) ACS Nano 4:43–48
14. Bae S, Kim H, Lee Y, Xu X, Park J, Zheng Y, Balakrishnan J, Lei T, Ri Kim H, Song YI, Kim Y, Kim KS, Ozyilmaz B, Ahn J, Hong BH, Iijima S (2010) Nat Nanotechnol 5:574–578
15. Lin YM, Dimitrakopoulos C, Jenkins KA, Farmer DB, Chiu HY, Grill A, Avouris P (2010) Science 327:662
16. Sutter PW, Flege J, Sutter EA (2008) Nat Mater 7:406–411
17. Tung VC, Allen MJ, Yang Y, Kaner RB (2009) Nat Nanotechnol 4:25–29
18. Novoselov KS, Geim AK, Morozov SV, Jiang D, Zhang Y, Dubonos SV, Grigorieva IV, Firsov AA (2004) Science 306:666–669

19. Reina A, Jia X, Ho J, Nezich D, Son H, Bulovic V, Dresselhaus MS, Kong J (2009) Nano Lett 9:30–35
20. Becerril HA, Mao J, Liu Z, Stoltenberg RM, Bao Z, Chen Y (2008) ACS Nano 2:463–470
21. Eda G, Fanchini G, Chhowalla M (2008) Nat Nanotechnol 3:270–274
22. Chen Y, Zhang X, Zhang D, Yu P, Ma Y (2011) Carbon 49:573–580
23. Moon IK, Lee J, Ruoff RS, Lee H (2010) Nat Commun 1:73
24. Shin H, Kim KK, Benayad A, Yoon S, Park HK, Jung I, Jin MH, Jeong H, Kim JM, Choi J, Lee YH (2009) Adv Funct Mater 19:1987–1992
25. Zhang K, Mao L, Zhang LL, On Chan HS, Zhao XS, Wu J (2011) J Mater Chem 21:7302–7307
26. Lotya M, King PJ, Khan U, De S, Coleman JN (2010) ACS Nano 4:3155–3162
27. Lomeda JR, Doyle CD, Kosynkin DV, Hwang W, Tour JM (2008) J Am Chem Soc 130:16201–16206
28. Yan J, Fan Z, Wei T, Qian W, Zhang M, Wei F (2010) Carbon 48:3825–3833
29. Su C, Xu Y, Zhang W, Zhao J, Liu A, Tang X, Tsai C, Huang Y, Li L (2010) ACS Nano 4:5285–5292
30. Yang X, Zhu J, Qiu L, Li D (2011) Adv Mater 23:2833–2838
31. Wang H, Zhang C, Liu Z, Wang L, Han P, Xu H, Zhang K, Dong S, Yao J, Cui G (2011) J Mater Chem 21:5430–5434